Available online at www.sciencedirect.com
ScienceDirect
Journal of Solid State Chemistry 181 (2008) 228–234
JOURNAL OF SOLID STATE CHEMISTRY
www.elsevier.com/locate/jssc

Crystal chemistry in the Ag_2O–Nb_2O_5 system $AgNb_3O_8$ structure determination

Patrick Rozier*, Olivier Szajwaj

Centre d'Elaboration de Matériaux et d'Etudes Structurales/CNRS, 29 Rue Jeanne Marvig, BP 94347, 31055 Toulouse Cedex, France

Received 9 August 2007; received in revised form 6 November 2007; accepted 12 November 2007
Available online 19 November 2007

Abstract

The investigation of the $AgNbO_3$–Nb_2O_5 system is carried out using solid-state routes. This investigation allows to confirm the existence of four compounds with structure related to the Na-based homologous. A new form of $AgNb_3O_8$ is evidenced and its structure is determined on the basis of single-crystal X-ray diffraction investigations. This compound crystallizes in the orthorhombic system (SG *Pbam*) with cell parameters $a = 12.453(4)$ Å; $b = 12.416(1)$ Å; $c = 3.9700(4)$ Å. It presents a TTB type host network in which triangular tunnels remain empty, square ones are fully filled with Ag^+ and pentagonal ones show mixed occupancy with Ag^+ and $[NbO]^{3+}$ entities. Crystal-chemistry investigations show that despite a complex and more or less disordered structure, no evidence for solid solution domain is observed.

Keywords: Crystal chemistry; TTB type structure; Silver niobium oxide system

1. Introduction

In the field of positive electrode materials for lithium batteries, silver- and copper-based compounds show, in addition to intercalation process, a displacement process in which Ag^+ and Cu^+ or Cu^{2+} are reduced to metal state and extrude out of the structure. Among the different reported compounds, $Cu_{7/3}V_4O_{11}$ and $Ag_2V_4O_{11}$ present a vanadium oxide layered host network [1]. Silver or copper cations, acting as guest species, connect to each other the VO layers [2,3]. A comparative study has demonstrated that only these two compounds present a full reversibility of the different mechanisms, opening the way for the design of new class of positive electrode materials [4].

Trying to define the crystal-chemistry parameters which govern such reversibility, we need to test a wide range of host networks. We decided to investigate first the lithium reactivity of compounds in the Ag- or Cu- NbO systems. Nb has been selected due to its crystal chemistry allowing oxygenated surroundings related to V ones and to its potentiality in the design of structural arrangement different from those of the vanadium oxides. Examination of reported data in the Ag_2O–Nb_2O_5 system shows that only $AgNbO_3$ structure [5] and high-pressure form of $AgNb_3O_8$ [6] are reported. In addition to these two well-characterized compounds, the similarities of Ag and Na crystal chemistry drove the authors to suggest that compounds in the Na_2O–Nb_2O_5 system should have their equivalent in the silver-based one [7]. Then, the XRD pattern obtained on samples prepared with the adequate Ag_2O/Nb_2O_5 ratios were attributed to the corresponding formula without any other structural details leading to four expected, but not characterized, compounds $Ag_2Nb_4O_{11}$, $Ag_2Nb_8O_{21}$, $AgNb_7O_{18}$ and $AgNb_{13}O_{33}$.

Prior to any study of the reactivity of silver niobates, we need to settle the data (stoichiometry and structure) in this system. The aim of this paper is to report the (re-)investigation of the $AgNbO_3$–Nb_2O_5 part of the binary system and to determine the structure of a new form of $AgNb_3O_8$.

2. Experimental

2.1. Synthesis routes

As a first step, in order to determine the right chemical process, we performed a synthesis using Ag_2O and Nb_2O_5.

*Corresponding author. Fax: +33 5 62 25 79 99.
E-mail addresses: rozier@cemes.fr (P. Rozier), szajwaj@cemes.fr (O. Szajwaj).

0022-4596/$ - see front matter © 2007 Elsevier Inc. All rights reserved.
doi:10.1016/j.jssc.2007.11.013

They are weighed in amounts calculated to prepare $AgNbO_3$ selected as reference material. After grinding, the mixture is heated in a platinum crucible at 400 °C. The resulting powder analysis shows that it is consistent with a mixture of $AgNbO_3$, silver metal and unreacted Nb_2O_5. Annealing at 1000 °C ensures the completeness of the reaction. To prevent the formation of silver metal, the same synthesis was performed using $AgNO_3$ instead of Ag_2O. At 400 °C the resulting sample corresponds to $AgNbO_3$. Comparison of samples obtained using Ag_2O and annealed at 1000 °C or $AgNO_3$ does not show differences. Then despite the spontaneous reduction of silver oxide before reaction with Nb_2O_5, as the synthesis is performed in air, there is no influence on the obtained product. All the syntheses have then been performed using Ag_2O.

The investigation starts with a broad exploration of different compositions selected to cover the $AgNbO_3$–Nb_2O_5 part of the Ag_2O–Nb_2O_5 system. In addition to the well-characterized $AgNbO_3$ and high-pressure form of $AgNb_3O_8$, reported results suggest the existence of $Ag_2Nb_4O_{11}$, $AgNb_7O_{18}$, $Ag_2Nb_8O_{21}$ and $AgNb_{13}O_{33}$. The syntheses are performed using ratio Ag_2O/Nb_2O_5 corresponding to these compositions. The reactants are weighed in stoichiometric amounts according to the expected compositions and taking into account their purity level. The mixture is ground in an agate mortar and placed in an alumina crucible covered with a platinum foil. Syntheses are performed in air at 500 °C followed by successive heat treatments up to the melting point. After each heat treatment, samples are ground and controlled using XRD.

2.2. Crystal growth

Once identified, the samples are heated up to their melting point (close to 1200 °C), cooled down slowly to 1000 °C and finally to room temperature at a rate corresponding to the furnace inertia. All the samples (apart from $Ag_2Nb_4O_{11}$) present a congruent melting as confirmed by the comparison of powdered samples obtained before melting and after grinding of the crystals. They present needle or platelet like shapes with size ranging from 0.04 to 1 mm and light yellow colour. Even though most of them present defects (twins …), some are selected for structure determination.

2.3. Powder X-ray diffraction investigation

The samples obtained after each heat treatment are controlled by means of powder X-ray diffraction using a Seifert 3000TT diffractometer with monochromatized Cu$K\alpha$ radiation ($\lambda = 1.5418$ Å). X-ray patterns are measured in the 5–55° 2θ range in a step scan mode with a counting time of 4 s and an angular step width of 0.02° 2θ.

Phase identification is done by comparison of experimental pattern with pattern reported in the ICDD database [8] or calculated using crystallographic data reported in ICSD database [9]. Determination of crystallographic system and cell parameters is carried out using Dicvol procedure [10], while refinement of cell parameters uses Celref software [11], both integrated in the Winplotr suite [12].

2.4. Single-crystal X-ray diffraction investigation

X-ray studies were carried out on a four-circle diffractometer Bruker Kappa-CCD (Apex II) working with a Mo$K\alpha$ ($\lambda = 0.7107$ Å) source. Data integration and reduction were carried out using EVALCCD software [13]. SIR 92 [14] was used to solve the structure by direct methods using a F^2 refinement method. The integrated data were refined using SHELXL-97 [15] suite of programs within WIN-GX [16].

3. Results and discussion

3.1. Phase identification in the $AgNbO_3$–Nb_2O_5 system

Fig. 1 shows the experimental XRD pattern of samples obtained after annealing at 1000 °C. Comparison with patterns reported in ICDD data base shows that 1/1; 1/4; 1/7 and 1/13 compositions lead to XRD patterns matching the reported ones for $AgNbO_3$, $Ag_2Nb_8O_{21}$, $AgNb_7O_{18}$ and $AgNb_{13}O_{33}$, respectively.

The XRD patterns obtained with samples corresponding to 1/3 and 1/2 compositions and annealed at 1000 °C are similar and cannot be identified using reported ones suggesting the existence of at least one new compound. To get a better understanding, the XRD patterns obtained at selected temperatures for 1/2 and 1/3 compositions are reported in Figs. 2 and 3, respectively. Their examination shows that up to 500 °C, in both cases, a mixture of $AgNbO_3$ and unreacted Nb_2O_5 is observed. In the 600–800 °C temperature range, the experimental pattern obtained for 1/2 composition is clearly different from that observed after annealing at 1000 °C (Fig. 1). Its comparison with XRD patterns reported in the ICDD database

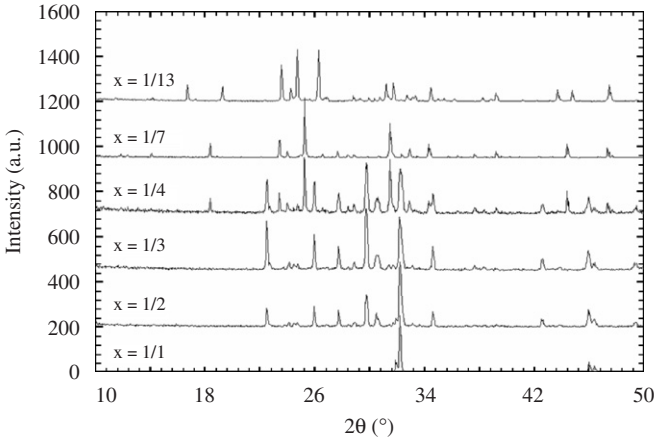

Fig. 1. Experimental XRD patterns for the different $x = Ag_2O/Nb_2O_5$ compositions annealed at 1000 °C.

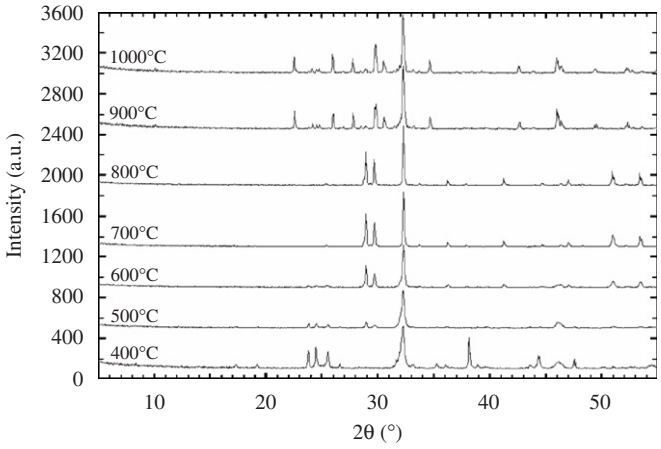

Fig. 2. XRD patterns obtained for 1/2 composition annealed at different temperatures.

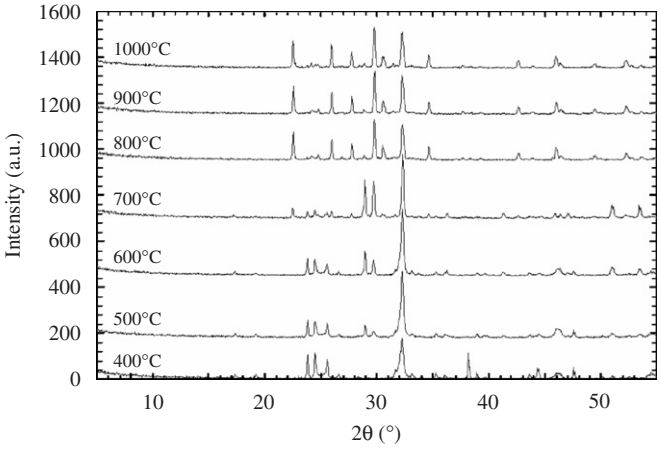

Fig. 3. XRD patterns obtained for 1/3 composition annealed at different temperatures.

shows that it matches the one reported for $Ag_2Nb_4O_{11}$. Above 800 °C, the decrease of the Bragg peaks characteristics of $Ag_2Nb_4O_{11}$ is observed together with the expanse of a new set of Bragg peaks matching the one observed at 1000 °C.

For 1/3 composition, at 600 °C, in the light of the latter experiments, the experimental pattern corresponds to a mixture of $Ag_2Nb_4O_{11}$ and unreacted Nb_2O_5. Above 700 °C, the reaction is completed leading to the XRD pattern observed at 1000 °C.

In addition to the well-characterized $AgNbO_3$ compound, this broad exploration confirms the existence of $AgNb_7O_{18}$ and $AgNb_{13}O_{33}$. It allows to specify that $Ag_2Nb_4O_{11}$ is stable only up to 800 °C. Upon further heating, it decomposes to form a mixture of $AgNbO_3$ and another compound which presents an XRD pattern close to that obtained with 1/3 composition. Both latter experiments suggest the existence of a new compound with formula $AgNb_3O_8$. Examination of XRD pattern obtained with 1/4 composition shows that it can be interpreted as a mixture of this new form of $AgNb_3O_8$ and $AgNb_7O_{18}$ instead of a compound with formula $Ag_2Nb_8O_{21}$.

3.2. Structural investigations

Except $AgNbO_3$, there are no structural data reported for the different compounds isolated in the $AgNbO_3$–Nb_2O_5 system. Previous studies have, however, shown that some similarities can be evidenced between Na- and Ag-based *M*–Nb–O compounds. On this basis, the structural data reported for $NaNb_{13}O_{33}$ [17], $NaNb_7O_{18}$ [18] and $Na_2Nb_4O_{11}$ [19] are used to index the experimental XRD patterns of the silver analogous and as starting model for cell parameters refinement.

The results are summarized in Table 1 and compared with reported ones for Na-based compounds. The agreement between patterns obtained experimentally and calculated using such refined cell parameters and considering that Ag ions replace Na ones in the prototype structure confirms that they can be considered as isostructural.

3.3. Single-crystal structure determination of $AgNb_3O_8$

To confirm and characterize the proposed new compound $AgNb_3O_8$, single crystals are prepared using 1/3 composition sample and following the process described in Section 2. All the single crystals selected exhibit defects which prevent for a precise structure determination. Such defects are well known to exist in the niobium-based oxides where extended defects like crystallographic shears or intergrowth have yet been observed. From the several single crystals tested, a needle ($0.1 \times 0.04 \times 0.04\,mm^3$) has a quality good enough to perform an accurate structure determination of the average structure and is used for data collection at room temperature. Operating conditions and X-ray crystallographic details are given in Table 2.

The cell parameters are determined from the collection of 40 diffraction peaks using the program EvalCCD [13]. The best fit leads to unit cell dimensions: $a = 12.453(4)$ Å; $b = 12.416(1)$ Å; $c = 3.9700(4)$ Å. The compound crystallizes in the orthorhombic system with space group *Pbam* (no. 55). The heavy Nb and Ag ions are located by direct methods and the oxygen ones by Fourier difference synthesis. The overall composition is calculated and corresponds to $AgNb_3O_8$ formula.

Table 1
Cell parameters for reported Na- and refined Ag-based compounds

Compound	Reference	SG	*a* (Å)	*b* (Å)	*c* (Å)	*β* (°)
$NaNb_{13}O_{33}$	[17]	*C*2/*m*	22.400	3.834	15.370	91.47
$AgNb_{13}O_{33}$		*C*2/*m*	22.378(1)	3.833(1)	15.394(1)	91.74(5)
$NaNb_7O_{18}$	[18]	*Immm*	3.8414	14.284	26.224	90
$AgNb_7O_{18}$		*Immm*	3.840(1)	14.315(1)	26.171(1)	90
$Na_2Nb_4O_{11}$	[19]	*C*2/*c*	10.810	6.162	12.741	106.22
$Ag_2Nb_4O_{11}$		*C*2/*c*	10.745(3)	6.201(2)	12.843(3)	106.18(2)

Table 2
Crystal data and structure refinement for $AgNb_3O_8$

Empirical formula	$AgNb_3O_8$	Crystal size	$0.1 \times 0.04 \times 0.04\,mm^3$
Formula weight	514.6	Theta range for data collection	6.09–26.33°
Temperature	293(2) K	Index ranges	$-11 \leqslant h \leqslant 15$, $-14 \leqslant k \leqslant 14$, $-4 \leqslant l \leqslant 4$
Wavelength	0.71073 Å	Reflections collected	2502
Crystal system	Orthorhombic	Independent reflections	558 [R(int) = 0.1301]
Space group	*Pbam*	Completeness to theta = 26.33°	78.2%
Unit cell dimensions	$a = 12.4530(11)$ Å	Absorption correction	Analytical
	$b = 12.416(4)$ Å	Maximum and minimum transmission	0.1241 and 0.0505
	$c = 3.9700(4)$ Å	Refinement method	Full-matrix least-squares on F_2
Volume	613.8(2) Å^3	Data/restraints/parameters	558/0/83
z	4	Goodness-of-fit on F_2	1.147
Density (calculated)	5.569 g cm^{-3}	Final R indices [$I > 2$sigma(I)]	$R_1 = 0.0790$, $wR_2 = 0.1933$
Absorption coefficient	8.609 mm^{-1}	R indices (all data)	$R_1 = 0.0984$, $wR_2 = 0.2028$
F(0 0 0)	936	Extinction coefficient	0.008(3)
		Largest diffraction peak and hole	2.097 and −2.457 e Å^{-3}

Table 3
Atomic coordinates and isotropic displacement parameters for $AgNb_3O_8$

	S.O.F.	x	y	z	U_{eq}[a]
Nb(1)	1	0.0759(2)	0.7089(1)	1/2	0.018(1)
Nb(2)	1	0.2910(1)	0.9248(3)	1/2	0.020(1)
Nb(3)	1/2	0.0173(6)	1.0157(9)	1/2	0.036(2)
Nb(4)	1/2	0.3369(8)	0.6675(7)	1/2	0.061(5)
Ag(1)	1	0	1/2	0	0.038(2)
Ag(2)	1/2	0.3242(8)	0.6717(8)	0	0.045(4)
O(1)	1	−0.006(3)	0.848(3)	1/2	0.05(1)
O(2)	1	−0.069(4)	0.627(4)	1/2	0.08(2)
O(3)	1	0.127(3)	0.565(3)	1/2	0.032(8)
O(4)	1	0.218(2)	0.783(2)	1/2	0.018(6)
O(5)	1	0.073(3)	0.707(3)	0	0.045(9)
O(6)	1	0.152(4)	1.004(4)	1/2	0.07(2)
O(7)	1	0.295(3)	0.930(3)	0	0.042(9)
O(8)	1/2	0.024(6)	0.029(5)	0	0.04(2)
O(9)	1/2	0.325(6)	0.704(7)	0	0.009(2)

[a] U_{eq} is defined as one-third of the trace of the orthogonalized U_{ij} tensor.

Table 4
Anisotropic displacement parameters (Å$^2 \times 10^3$) for $AgNb_3O_8$

	U_{11}	U_{22}	U_{33}	U_{23}	U_{13}	U_{12}
Nb(1)	0.012(2)	0.003(1)	0.042(2)	0	0	0.002(1)
Nb(2)	0.017(2)	0.005(1)	0.042(2)	0	0	−0.001(1)
Nb(3)	0.012(7)	0.004(6)	0.095(6)	0	0	0.003(4)
Nb(4)	0.034(5)	0.022(4)	0.123(9)	0	0	−0.007(3)
Ag(1)	0.058(3)	0.031(2)	0.029(2)	0	0	0.001(2)
Ag(2)	0.073(4)	0.044(5)	0.022(3)	0	0	−0.029(5)
O(1)	0.05(2)	0.02(1)	0.06(2)	0	0	0.02(1)
O(2)	0.02(1)	0.15(4)	0.07(2)	0	0	−0.03(2)
O(3)	0.17(4)	0.02(1)	0.07(2)	0	0	0.03(2)
O(4)	0.05(2)	0.01(1)	0.04(2)	0	0	−0.02(1)
O(5)	0.04(2)	0.07(2)	0.04(2)	0	0	0.02(1)
O(6)	0.02(1)	0.01(1)	0.10(2)	0	0	0.007(9)
O(7)	0.06(2)	0.04(2)	0.04(2)	0	0	0
O(9)	0.073(4)	0.044(5)	0.022(3)	0	0	−0.029(5)

The anisotropic displacement factor exponent takes the form: $-2\pi^2[h^2 a^* \times 2U_{11} + \cdots + 2hk a^* \times b^* \times U_{12}]$.

Table 5
Selected bond lengths (Å) for $AgNb_3O_8$

Nb(1)–O(1)	2.00(2)	Nb(2)–O(2)$^{\#1}$	1.86(3)	Nb(3)–O(1)	2.10(3)
Nb(1)–O(2)	2.07(3)	Nb(2)–O(3)$^{\#2}$	2.03(3)	Nb(3)–O(1)$^{\#3}$	1.70(2)
Nb(1)–O(3)	1.89(3)	Nb(2)–O(4)	1.98(2)	Nb(3)–O(6)	1.69(3)
Nb(1)–O(4)	1.99(2)	Nb(2)–O(6)	1.99(2)	Nb(3)–O(6)$^{\#3}$	2.12(3)
2 × Nb(1)–O(5)	1.98(6)	2 × Nb(2)–O(7)	1.98(1)	2 × Nb(3)–O(8)	1.99(5)
				2 × Nb(3)–O(8)$^{\#3}$	2.11(2)
Nb(4)–O(1)	1.98(3)	4 × Ag(1)–O(2)	2.68(3)	2 × Ag(2)–O(1)$^{\#1}$	2.90(2)
Nb(4)–O(4)	2.07(2)	4 × Ag(1)–O(3)	2.67(3)	2 × Ag(2)–O(4)	2.76(2)
Nb(4)–O(6)$^{\#2}$	2.03(2)	2 × Ag(1)–O(5)	2.73(3)	2 × Ag(2)–O(6)$^{\#2}$	2.87(2)
2 × Nb(4)–O(9)	2.04(2)	2 × Ag(1)–O(7)	2.72(3)	Ag(2)–O(8)$^{\#2}$	2.65(5)
Nb(4)–O(2)	2.75(3)				
Nb(4)–O(3)	2.86(3)				

Symmetry operators: (#1) 1/2 + x; 1/2−y; 1−z; (#2) 1/2−x; 1/2 + y; −z; (#3) −x; −y; z.

Final atomic coordinates and isotropic thermal parameters are given in Table 3. Anisotropic thermal displacement parameters are listed in Table 4 while a selection of interatomic bond lengths is gathered in Table 5. The final refinement converges to R-values: $R_{obs} = 7.90\%$ for 440 reflections ($I > 2\sigma(I)$) and $R_{all} = 9.84\%$ for all the 558 reflections, with 83 parameters refined using no restraint. The relatively high reliability factors traduce the presence of extended defects. Despite several tests, all attempts to enhance the crystallinity were unsuccessful. Nevertheless, data are accurate enough to allow us to settle the structure of this new form of $AgNb_3O_8$ and to give pertinent reasons explaining the relatively high reliability factor.

Nb(1), Nb(2), Nb(3), located in the $z = 1/2$ plane, present a more or less distorted octahedral oxygenated surrounding (Fig. 4). These polyhedra share corners to form the well-known TTB structure (Fig. 5) defining three kinds of tunnels differing by their form. The triangular ones are empty, while Ag(1), located in the $z = 0$ plane, in a cube–octahedron oxygenated surrounding (Fig. 6a) fill the square ones. The occupancy of the pentagonal ones is a little bit more complicated to describe. The distribution of the electronic densities in this pentagonal tunnel shows two maxima at $z = 0$ and $z = 1/2$ (Fig. 7). In agreement with other heavy atoms location and with respect to conventional M–O distances, the density located at $z = 1/2$ is attributed

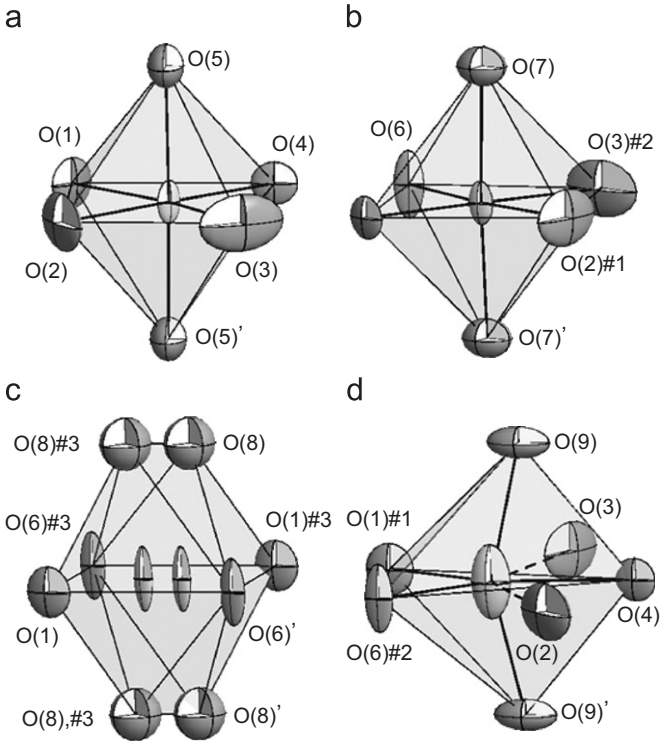

Fig. 4. Nb oxygenated surroundings in $AgNb_3O_8$ structure.

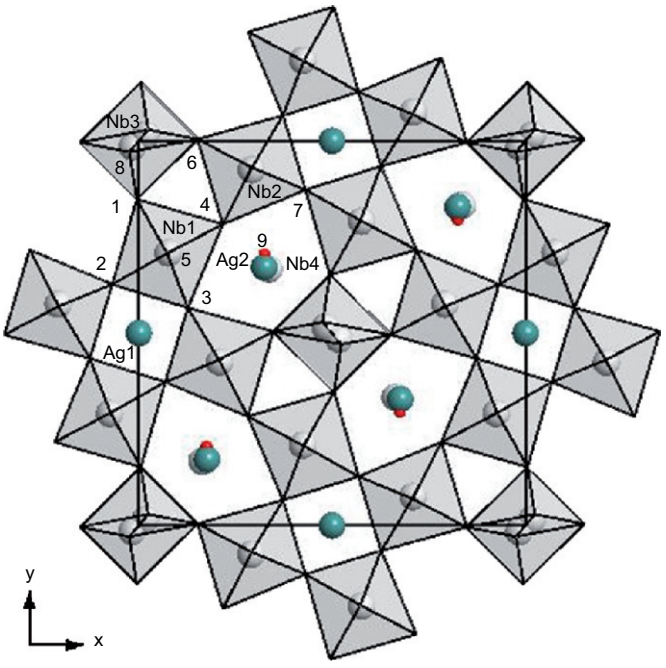

Fig. 5. Projection onto the (0 0 1) plane of the $AgNb_3O_8$ structure.

to an extra Nb contribution (Nb(4)), while the one located at $z = 0$ is assumed to be related to an extra Ag contribution (Ag(2)). Taking into account these contributions a Fourier difference map shows residual electronic density in the $z = 0$ plane. It has been attributed to an extra oxygen ion (O(9)) which completes the surrounding Nb(4). The short Nb(4)–Ag(2) distance (1.985 Å) implies that these sites cannot be occupied simultaneously. The occupancy of these sites is restricted to 1/2 and refined. The refinement rapidly converges to a value close to 1/2. As the observed differences are in accuracy limit, occupancies are fixed to 1/2.

Ag(2) is located in a regular monocapped trigonal prism (Fig. 6b), while Nb(4) is five-fold coordinated in a trigonal bipyramid (Fig. 4d). This latter surrounding can be extended up to a pentagonal bipyramid taking into account two large Nb–O distances (2.75 and 2.86 Å). The mixed occupancy of the pentagonal tunnels by alternative Nb(4)–O(9) entity or Ag(2) cation is the reason for $Nb(3)O_6$ octahedron distortion. In the former case, the minimization of the repulsive character of the Nb(3)–Nb(4) interaction is responsible for the movement of Nb(3) out of the centre $(0\,0\,\frac{1}{2})$ of its octahedron to the $(x\,y\,\frac{1}{2})$ position and of the associated apical oxygen O(8) from (0 0 0) to $(x\,y\,0)$. This induces an increase up to 3.19 Å of the distance between adjacent Nb(3) and Nb(4) ions in agreement with conventional Nb–Nb distances. This repulsive effect drives also to a decrease of the distance between Nb(3) and the centre of the next pentagonal tunnel (2.61 Å) implying that it cannot be occupied by another Nb(4) ion but only by an Ag(2) cation lying in the $z = 0$ plane. The Nb(3)–Ag(2) distance equal to 3.40 Å is then in agreement with conventional ones. These phenomena lead to a specific Nb(4)–Nb(3)–Ag(2) ordering represented in Fig. 8. The distribution of these entities is found statistical in the average structure. However, ordered distribution can occur and would induce superstructure, or extended defects explaining the relatively high R factors.

3.4. Study of a possible solid solution of $AgNb_3O_8$

The similarity of "high temperature" 1/2 and 1/3 XRD patterns suggests the existence of a solid solution. The determination of the structure of $AgNb_3O_8$, a member of this suspected solid solution, allows then to propose structural parameters that encounter for a change in composition. $AgNb_3O_8$ presents the typical TTB structure in which the host network $[Nb_{10}O_{30}]^{10-}$ defines three kinds of tunnels, and among them the triangular ones remain empty. Ag^+ lies in both square (Sq) and pentagonal (Pe) tunnels, while $(NbO)^{3+}$ lies only in the pentagonal ones. The combination of both occupancy and charge compensation rules allows to define the general formula:

$$[(NbO)_aAg_b]_{Pe}[Ag_c]_{Sq}[Nb_{10}O_{30}]$$

with the restrictions:

$$a \times 3 + b \times 1 + c \times 1 = 10;$$
$$0 < a < 4; \quad 0 < b < 4 \quad \text{with} \quad a + b < 4;$$
$$0 < c < 2.$$

This equation is solved for values between ($a = 10/3$; $b = c = 0$) and ($a = 2$; $b = 2$; $c = 2$) meaning between $[(NbO)_{10/3}]_{Pe}[Nb_{10}O_{30}] = Nb_{40}O_{100}$, i.e. Nb_2O_5 for the lowest silver content and $[(NbO)_2Ag_2]_{Pe}[Ag_2]_{Sq}[Nb_{10}O_{30}) = Ag_4Nb_{12}O_{32}$, i.e. $AgNb_3O_8$ for the highest silver content.

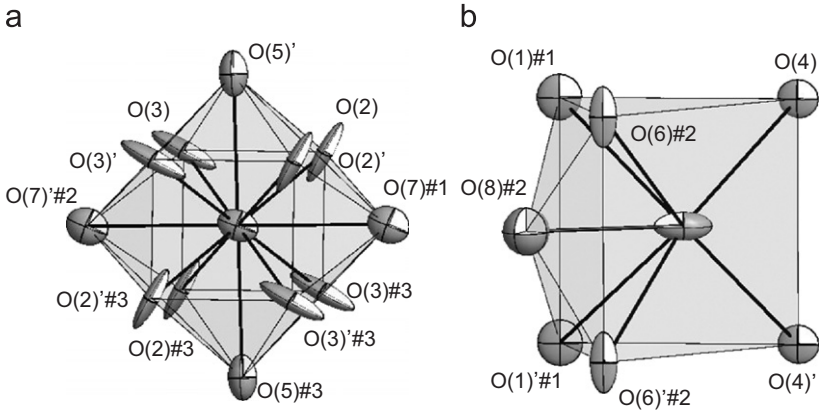

Fig. 6. Silver oxygenated surroundings in $AgNb_3O_8$ structure.

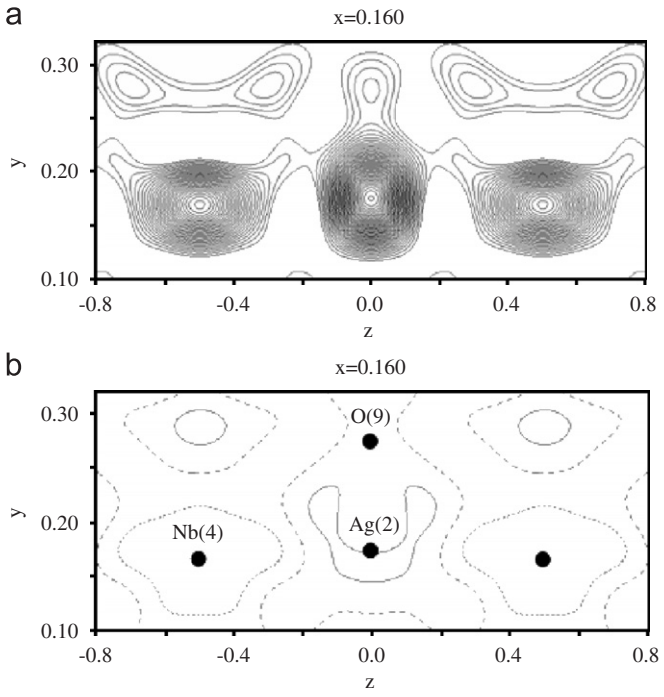

Fig. 7. Electronic density observed (a) without and (b) with Nb(4), Ag(2) and O(9) contributions.

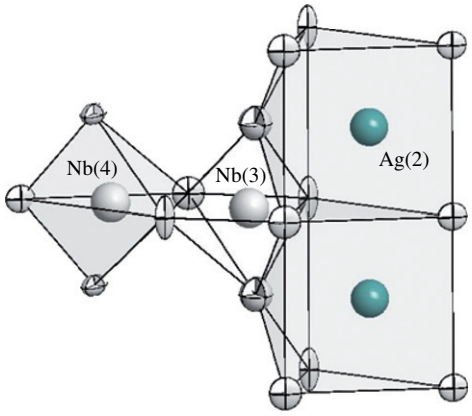

Fig. 8. Proposed ordered occupancy for Nb(4)–Nb(3)–Ag(2) in $AgNb_3O_8$ structure.

Unambiguously for both occupancy and charge balance reasons, the upper limit of such a solid solution is $AgNb_3O_8$ (1/3 composition). Then, the XRD pattern of high-temperature form of 1/2 composition ($Ag_2Nb_4O_{11}$), even though similar to that of $AgNb_3O_8$, corresponds to the mixture generated by the decomposition mechanism: $Ag_2Nb_4O_{11} \rightarrow AgNb_3O_8 + AgNbO_3$.

Formally such solid solution can be extended down to Nb_2O_5. However, as detailed above, the screening of the Ag_2O–Nb_2O_5 system shows that $AgNb_{13}O_{33}$ and $AgNb_7O_{18}$ present structural arrangement different from that of TTB. This can be interpreted as the necessity, to stabilize the TTB structure, to fully fill the square tunnels with silver. In such a case, the lower limit should correspond to $[Ag_2Nb_{10}O_{30}]^{8-}$. The remaining eight charges have to be compensated using 8/3 NbO^{3+} entities leading to $[(NbO)_{8/3}]_{Pe}[Ag_2]_{Sq}[Nb_{10}O_{30}] = Ag_6Nb_{38}O_{98}$, i.e. $Ag_3Nb_{19}O_{49}$. This 3/19 composition lies in between the 1/4 and 1/7 ones. However, our study shows that 1/4 composition is a mixture between $AgNb_3O_8$ and $AgNb_7O_{18}$. That means that the studied solid solution does not extend down to the 1/4 composition and so should not be extended down to 3/19 one. A synthesis is performed in the last part of the binary system between 1/3 and 1/4. The selected composition is 2/7 which corresponds to the middle of this segment. Clearly after different heat treatments at increasing temperatures, the sample is characteristic of a mixture of $AgNb_3O_8$ and $AgNb_7O_{18}$.

From these studies, we can unambiguously confirm that $AgNb_3O_8$ corresponds to a defined compound. Even speculations about some ordering in the occupancy of the different tunnels of the TTB type network does not lead to evidence any other compound related to $AgNb_3O_8$ structure type. This contradiction between possibilities to perform a solid solution and the existence of only a defined compound can be understood by the use of another way of description of the $AgNb_3O_8$ structure or, more precisely, the way one can fill the pentagonal tunnels. Going back to the evidence that TTB structure is stabilized only when square tunnels are fully occupied, the formula is $[Ag_2Nb_{10}O_{30}]^{8-}$.

As we know that pentagonal tunnels can be filled with Ag or NbO entities, two ending members corresponding to the occupancy with only Ag or only NbO can be calculated leading to the formula $[Ag_4Ag_2Nb_{10}O_{30}]^{4-}$ and $[(NbO)_4Ag_2Nb_{10}O_{30}]^{4+}$, respectively. The only way to form a neutral compound is then to mix equivalent amount of each ending compounds following:

$$[Ag_6Nb_{10}O_{30}]^{4-} + [Ag_2Nb_{14}O_{34}]^{4+} \rightarrow Ag_8Nb_{24}O_{64}, \text{ i.e. } AgNb_3O_8.$$

In such a latter case, $AgNb_3O_8$ could be considered as an intergrowth of $Ag_6Nb_{10}O_{30}$ and $Ag_2Nb_{14}O_{34}$. Usually ordered on a more or less large distance, the investigation by XRD cannot allow to evidence such intergrowths but the difficulties encountered during the structure determination can be indicative of the effectiveness of such process.

4. Conclusion

The screening of composition with Ag_2O/Nb_2O_5 ratio ranging from 1/1 to 1/13 allows us to identify and characterize four compounds in addition to the well-known $AgNbO_3$ perovskite type one and the high-pressure form of $AgNb_3O_8$.

1/13, 1/7 and 1/2 compositions lead to compounds with formula AgNb13O33; $AgNb_7O_{18}$ and $Ag_2Nb_4O_{11}$, respectively. Their structure, as suggested in previous studies, is related to the Na-based homologous. $Ag_2Nb_4O_{11}$ is stable only in the 600–800 °C temperature range and decomposes into a $AgNbO_3/AgNb_3O_8$ mixture above 800 °C. The structure of this latter compound determined by means of single-crystal XRD is related to the TTB family. The charge compensation implies statistical occupancy of the pentagonal tunnel by alternative silver cations and NbO entities while the square tunnels are filled with Ag^+ and triangular ones remain empty. The 1/4 composition reported in the literature as a compound $Ag_2Nb_8O_{21}$ does not exist and corresponds to a mixture of $AgNb_7O_{18}$ and $AgNb_3O_8$. The compilation of all these results allows to settle the compounds present in the niobium-rich part of the Ag_2O–Nb_2O_5 system. The structure of the different compounds is determined by refinement of Na-based homologous or by means of XRD on single crystal.

References

[1] P. Rozier, C. Satto, J. Galy, Solid State Sci. 2 (6) (2000) 595–606.
[2] R. Withers, P. Rozier, Z. Kristallogr. 215 (2000) 688–692.
[3] P. Rozier, S. Lidin, J. Solid State Chem. 172 (2003) 319–326.
[4] M. Morcrette, P. Rozier, L. Dupont, E. Mugnier, L. Sannier, J. Galy, J.-M. Tarascon, Nat. Mater. 2 (2003) 755–761.
[5] J. Fabry, Acta Crystallogr. Sect. C 56 (8) (2000) 916–918.
[6] K.J. Range, ZNBSEN 44 (1989) 499–501.
[7] H.G.P. Brusset, J.-P.H. Belle, Bulletin de la Société Chimique Franç aise, 1967.
[8] International Centre for Diffraction Data, 2007.
[9] Inorganic Crystal Structure Database, National Institute of Standards and Technology, 2007.
[10] A. Boultif, D. Louer, J. Appl. Crystallogr. 37 (2004) 724–731.
[11] D. Altermatt, I.D. Brown, Acta Crystallogr. A 34 (1987) 125–130.
[12] T. Roisnel, J. Rodríguez-Carvajal, Mater. Sci. Forum EPDIC 7 (2000) 118–123.
[13] Bruker, Collect and EvalCCD, B.A. Inc., Madison, WI, 2002.
[14] A. Altomare, J. Appl. Crystallogr. 27 (3) (1994) 435.
[15] G.M. Sheldrick, SHELX-97: a program for crystal structure refinement, 1997.
[16] L.J. Farrugia, J. Appl. Crystallogr. 32 (1999) 837.
[17] S. Andersson, Acta Chem. Scand. 19 (1965) 557–563.
[18] B.O. Marinder, M. Sundberg, Acta Crystallogr. Sect. B 40 (2) (1984) 82–86.
[19] L. Jahnberg, J. Solid State Chem. 1 (1970) 454–462.